SISSA

PAPER • OPEN ACCESS

Performance of a thick 250 µm silicon carbide detector: stability and energy resolution

View the article online for updates and enhancements.

Performance of a thick 250 μm silicon carbide detector: stability and energy resolution

M.H. Kushoro,[a,b,*] **M. Rebai,**[b] **F. La Via,**[c] **A. Meli,**[c,e] **L. Meda,**[d] **M. Parisi,**[d] **E.P. Cippo,**[b] **O. Putignano,**[a,b] **A. Trotta**[d] **and M. Tardocchi**[b]

[a]*Dipartimento di Fisica "G. Occhialini", Università di Milano-Bicocca,*
20126 Milano, Italy

[b]*Istituto per la Scienza e Tecnologia dei Plasmi, Consiglio Nazionale delle Ricerche,*
20126 Milano, Italy

[c]*Institute for Microelectronics and Microsystems, Consiglio Nazionale delle Ricerche,*
VIII Strada, 5, 95121 Catania, Italy

[d]*ENI S.p.A. CENTER—Renewable Energy & Environmental R & D, 28100 Novara, Italy*

[e]*Università di Catania, 95123 Catania, Italy*

E-mail: m.kushoro@campus.unimib.it

ABSTRACT: Silicon carbide detectors represent an alternative to diamond detectors for fast neutron detection in harsh environments, especially fusion plasmas. Previous studies on thin prototypes (either 10 μm or 100 μm thick) suggested that thicker active volumes might be better suited for spectroscopy measurements, due to the higher chance of retaining the neutron interaction products inside the active volume. Therefore, in this work two 250 μm SiC prototypes are tested with alpha particles following the same process conducted in the past for thinner prototypes. A stable detection is demonstrated, along an energy resolution that, if projected to DT neutrons, could become the lowest achieved so far with a SiC detector (1.3%). Some difficulties in reaching a full depletion are highlighted, as long as perspectives of a partial polarization operation of the detectors.

*Corresponding author.

Contents

1   Introduction

Solid State Detectors (SSD) are object of interest in the field of fast neutron detection and spectroscopy in tokamaks [1]. Their solid structure, ability to discriminate neutrons from gamma radiation [2] and insensitivity to magnetic field makes them prime candidates for neutron detection close to the plasma [3]. Furthermore, the fact that their detection mechanism doesn't rely on a conversion stage outside the active volume allows for very low energy resolutions. In perspective, their small dimensions also allow for their installation in arrays enabling the survey of the tokamak volume along multiple lines of sight [4]. There are also solid prospects for the functionality of SiC in harsh environments (such as high temperature [5, 6] or high radiation [7–10]) such as the one encountered inside the breeding blanket (or, in general, close to the plasma).

There is abundant research on both silicon and diamond SSDs, enshrining the latter as the state of art for SSDs fast neutron detection [4, 11–17]. The silicon carbide detector (SiC), on the other hand, has received less coverage: while it combines the reaction channel of both silicon and carbon (leading to a more complicated response of the detector [18, 19]) there is a larger experience on manufacturing SiC wafers up to 200 mm in diameter with a low degree of defects, allowing for purer and cheaper detectors when compared to diamond (the maximum dimension of which is about $5 \times 5 \, \text{mm}^2$). SiC has also been proven more stable than diamond [20], since the latter has been proven to experience a loss of counts over prolonged irradiation due to a polarization effect [21, 22]. There are also more solid perspectives for high temperature operation for the SiC [6, 23] than the diamonds [5, 24, 25]: this drives the interest on furthering the research on the SiC as a fast neutron detector for fusion plasma harsh environments [7, 26].

2   Detectors and scope

Silicon carbide active volume is made by a hexagonal lattice of 50% silicon and 50% carbon, grown by the means of CVD technique [27] on a substrate. Contrarily to diamond detectors (which are intrinsic semiconductors), the SiC is structured as an inversely polarized p–n junction in which a depletion region is formed by applying a reverse bias. The interaction of a neutron on

an atom of the lattice inside the depletion region creates ions and/or charged particles (depending on the type of reaction triggered) which are slowed down inside the lattice, generating a number of electron-hole pairs proportional to the energy deposited by the neutron (E_d). Those pairs are separated by the electric field in the diode generating a current pulse proportional to E_d, which can be read at the two electrodes of the active volume.

Some prototypes of silicon carbide were tested in the past under neutron and alpha particle irradiation (while the interest in the detection of the latter is marginal, alphas are used as a more manageable, easy-to-handle calibration source). The prototypes were manufactured through a collaboration between INFN and IMM-CNR [26, 27]. The detectors are grown by the means of CVD technique, having active volumes of either 10 μm or 100 μm thickness and area of the single detector between $12.5\,\text{mm}^2$ and $25\,\text{mm}^2$. They feature a 0.3 μm p-layer with a doping concentration between 10^{18} and 10^{19} cm^{-3}, and a n-layer with a doping concentration of 8×10^{13} cm^{-3} [26]. Their functionality was demonstrated [18] with a 2.7% energy resolution to 14 MeV neutrons [19] and 2.9% to 4.3 MeV alpha particles [20] with a detection stability exceeding by at least two orders of magnitude the limited stability of diamond [21]. The efficiency to neutrons was proven proportional to the active volume size (6×10^{-4} for a 5 mm × 5 mm × 100 μm SiC to 14 MeV neutrons) [18]: the very low efficiency is, perhaps counterintuitively, a feature, since future tokamak DT experiments will be characterized by very high neutron fluences which would saturate a detector with a higher efficiency.

On the other hand, low thicknesses experience more often the loss of the charged products of the neutron interaction before they deposit their entire energy E_d, severely hampering spectroscopic capability [28, 29]. This is true for both SiC10 and SiC100: in fact, one of the most interesting reaction channels for 14 MeV neutrons is $^{12}\text{C}(n, \alpha)^9\text{Be}$, producing a 5.75 MeV alpha particle [30] which has a range in SiC of about 18.86 μm (path which is comparable with the SiC thicknesses). This range was obtained by averaging the projected range for carbon (16.20 μm) and silicon (21.52 μm) through the continuous slowing down approximation, as obtained from the ASTAR NIST catalogue [31] assuming a SiC density of 3.22 g/cm^2 [27]. Considering this, a relevant percentage of high-E_d products in the SiC100 (and a vast majority of high-E_d products in the SiC10) will escape the lattice before depositing their energy, hampering the energy resolution and the detection quality. This is part of the reason by which the absolute value of the energy resolution to 14 MeV neutrons (14 MeV × 2.7% = 378.0 keV [19]) is higher than the absolute value to 4.3 MeV alphas (4.3 MeV × 2.9% = 124.7 keV [20]).

This consideration drove the interest toward thicker SiC detectors. A new series of prototypes of thickness 250 μm ("SiC250") were developed in the same collaboration above though the same CVD technique and with similar doping [32]. The new thickness brought forward some unprecedented requirements for the polarization required to fully deplete the active volume. In fact, the depletion region extends parallelly to the surface of the active volume to a depth d as a function of the bias potential V. From [33]:

$$d \simeq \sqrt{\frac{2\varepsilon_{\text{SiC}}}{eN_A} \cdot V}$$

By substituting the dielectric constant of the silicon carbide $\varepsilon_{\text{SiC}} = 8.633 \times 10^{-11}\ \frac{\text{C}^2}{\text{N m}^2}$, the electron charge $e = 1.602 \times 10^{-19}$ C, the n-layer doping concentration $N_A = 8 \times 10^{13}$ cm^{-3} and

reversing the equation, we obtain that the potential needed to fully deplete the 250 µm active volume is 4600 V. Such high voltage is unachievable at present date, due to the limits imposed by the preamplifier; as such, it was chosen to conduct a preliminary alpha particle irradiation on a partially polarized SiC in order to test its functionality, obtain the energy resolution of the new detector and evaluate its stability, similarly to what was performed in [20]. Since the alpha particle source chosen was an americium-241 source (emitting alphas with energy $E_\alpha = 5.49$ MeV, which are then slowed down in air) a 100 V bias was chosen in order to deplete 36.7 µm of the detector, which is deep enough to fully stop the alpha particles.

3 Experimental setup

The detectors and the electronic chain are depicted in figure 1. Two different SiC250 prototypes, named SiCD and SiCE, are installed in aluminum casings connected with the ground, acting as a Faraday cage. Each of the detectors is connected to a Cividec SiC Amplifier [34], which was developed on the specific characteristics of the SiC. The preamplifier conveys the supplied HV to the detector and amplifies the signal obtained, forming it into a 100 ns long semi-Gaussian shape. The signal is then read by a CAEN 5730 analog to digital converter [35] which identifies events through a threshold-over-baseline method.

Figure 1. Experimental setup. On the right the three SiC detectors are shown inside their aluminum casing (from top to bottom: SiCD, SiCE and a third SiC, not used in this work). The bottom SiC is connected to the Cividec Preamplifier, powered by a 12 V power source (blue cable at the bottom) and supplying the detector the bias tension (top cable). The middle cable feeds the signal, shaped by the preamplifier, to the CAEN 5730 ADC (on the right). The electrodeposited ^{241}Am source (on top, inside the red box) is put on the top of the aluminum casings, the holes in which allows alphas to reach the active volumes beneath.

The irradiation source is an electrodeposited ^{241}Am source moderated in air. The Americium decay produces a constant flux of 5.49 MeV alpha particles, which are slowed down in the air between the source and the surface of the detector. By measuring the distance and the stopping power of air [31] the energy of the alpha interacting with the SiC was calculated for each of the detectors: 4.17 MeV for the SiCD and 4.69 MeV for the SiCE. The path in air of all alpha particles was assumed constant, due to:

- The alpha particle flux was conveyed through a hole in the aluminum casing, allowing for a collimation of the particles.

- The ratio between the mean total path within the CSDA approximation and the projection along the direction of emission of the alpha particles is 0.9925 [31]: since the two values are equal within a 1% uncertainty, the straggling can be neglected, and all alpha particles can be assumed to walk a straight path.

Following the same process performed in [20] the signals detected were grouped up in five-minute spectra, on which a gaussian fit favouring the higher energies of the gaussian (the right side) was performed. From the fit three information are extracted:

- Number of counts every five minutes, which is proportional to the detector efficiency to alphas.

- Center value of the gaussian, which gives information about the response function.

- Full width at half maximum of the gaussian (FWHM), obtained from the σ of the gaussian fit via FWHM $= 2\sqrt{2 \cdot \ln 2} \cdot \sigma$.

Such information is computed every five minutes along all the irradiations for each of the two detectors and plotted as a function of time. The two irradiations lasted for 72 h and 86 h, consisting in alpha fluences up to $\phi \simeq 9.2 \times 10^7$ cm^{-2}. The goal is to demonstrate the stability of the detection by proving that the three quantities above do not change as a function of time and irradiation. By dividing the FWHM by the center value of the Gaussian, a first estimate of the energy resolution of the setup (SiC250 + new preamplifier) can be obtained.

4 Results

The value of the number of counts, center value of the Gaussian and energy resolution obtained in every five-minute interval is plotted in figure 2. The absence of drifts in all three quantities for both detectors proves the detection stability. The only visible drift is the SiCE pulse height, which slightly declines by about 1.5% in the region between 200000 seconds to 250000 second ($\simeq$14 hours); the fact that the drift is comparatively small and has no analogue in the other quantities suggests it could be due to changes in the air stopping power due to humidity or temperature shifts rather than actual variation in the response function of the detectors.

By taking the mean value of the energy resolution we can obtain the energy resolution of the two detectors, which is reported in the table below. In the same table is also reported the FWHM and the projected value of energy resolution to 14 MeV neutrons if the same FWHM (and, thus, the absolute value of the energy resolution) is kept the same. The same values for SiC100 from [20] are also reported, paired with the energy resolution to 14 MeV neutrons obtained through experiment [19].
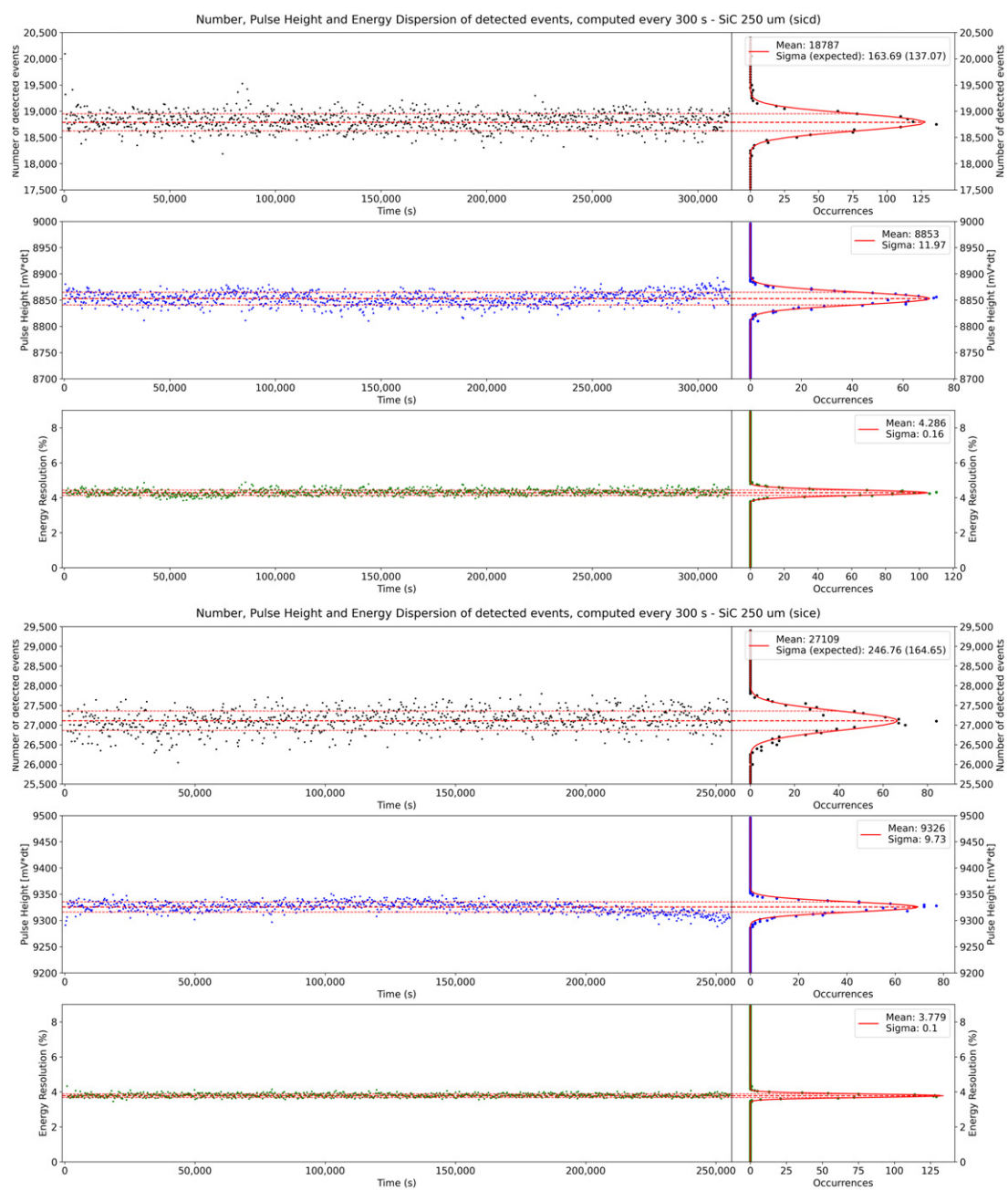
Figure 2. Time evolution of the number of counts (black), the mean pulse height (blue) and the energy resolution (green) for the two SiC250, SiCD (top) and SiCE (bottom), under irradiation of monochromatic alpha particles (4.17 MeV and 4.69 MeV respectively). Each of the points correspond to a 300 s ensemble. On the right, the dispersion of the data is projected on the *y*-axis, computing the mean value of the three quantities along with its standard deviation. For the number of counts the standard deviation is compared to the expected dispersion due to statistical error (equal to the square root of the number of counts). The figure is the direct analogue of figure 3 from [20] for the SiC250.

Detector name	Energy resolution (alpha energy)	Full width at half maximum	Projected value of energy resolution to 14 MeV neutrons
SiCD	4.30% (4.17 MeV)	179.31 keV	1.28%
SiCE	3.80% (4.69 MeV)	178.22 keV	1.27%
			En. Res. to 14 MeV Neut. (experiment)
SiC100	2.89% (4.3 MeV) [20]	124.7 keV [20]	2.7% [19]

The energy resolution to alphas obtained for both detectors is higher (and, thus, worse) than the 2.89% value obtained on the SiC100 (corresponding to a FWHM = 124.7 keV). In order to exclude the possibility of the higher energy resolution being due to the new preamplifier 30 minutes irradiations were performed with the same setup and the preamplifier used in [19], yielding an energy resolution of 4.57% (for the SiCD). The worst performance, therefore, could be due to dark currents flowing inside the active volume adding to the integral of the signal and therefore broadening its spectrum. Such currents are presumably due to trapped charges into crystal defects [36], which are expected to be more common in thicker SiCs [32, 37].

5 Conclusions

Two prototypes of silicon carbide detector with unprecedented thicknesses (250 μm) were tested with monoenergetic alpha particles. Their stability to fluences up to $\phi \simeq 9.2 \times 10^7$ cm^{-2} were proven by verifying the invariability of counting efficiency, response function and energy resolution along a two to three days irradiation to monoenergetic alpha particles: this confirms that SiC250 prototypes share the same good stability of the 10 μm and 100 μm counterparts assessed in [20]. The energy resolution to alphas obtained was nearly equal for two prototypes (around 179 keV FWHM, resulting in a 3.8% energy resolution to 4.69 MeV alphas and 4.3% resolution to 4.17 MeV alphas). Both resolutions are higher than the one demonstrated with a 100 μm SiC in [20]: this could be due to dark currents flowing inside the 250 μm detectors, possibly due to a higher density of defects and charge-trapping sites.

Nevertheless, if the FWHM of the detectors can be maintained to 14 MeV neutrons, the two thick SiCs coupled with the new electronics could reach a 1.27% energy resolution, which would be unprecedented for the SiC, putting them almost on par with the best energy resolutions achieved with diamonds (1% [14]). This would require very high bias voltages (4600 V) to fully deplete the thick crystals, which is unreachable with the current electronics. The functionality proven in this paper, though, suggests that it is possible to use the detectors even with a partial depletion region, which would allow for an online tuning of the size of the active volume, and therefore the efficiency of the detector. This might prove also a feature for high temperature operation, where lower biases have been demonstrated to be more suitable for the detection [6, 23]. All these perspectives will be analyzed in an upcoming work.

References

[1] G. Ericsson, *Advanced neutron spectroscopy in fusion research, J. Fusion Energy* (2019) **38** 330.

[2] F.H. Ruddy et al., *Development of a silicon carbide radiation detector, IEEE Trans. Nucl. Sci.* **45** (1998) 536.

[3] J.M. Gómez-Ros, *Solid state detectors for neutron radiation monitoring in fusion facilities, Radiat. Meas.* **71** (2014) 421.

[4] M. Tardocchi et al., *High rate neutron and gamma ray spectroscopy of magnetic confinement fusion plasmas,* 2020 *JINST* **15** C01010.

[5] C. Weiss et al., *High-temperature performance of solid-state sensors up to 500 °C, Nucl. Instrum. Methods Phys. Res., Sect. A* **1040** (2022) 167182.

[6] D. Szalkai et al., *Fast neutron detection with 4H-SiC based diode detector up to 500 °C ambient temperature, IEEE Trans. Nucl. Sci.* **63** (2016) 1491.

[7] F. La Via, *Silicon carbide devices for radiation detection and measurements, J. Phys.: Conf. Ser.* **1561** (2020) 012013.

[8] A. Owens, & A. Peacock, *Compound semiconductor radiation detectors, Nucl. Instrum. Methods Phys. Res., Sect. A* **531** (2004) 18.

[9] E.V. Kalinina et al., *Performance of p–n 4H-SiC film nuclear radiation detectors for operation at elevated temperatures (375 °C), Tech. Phys. Lett.* **34** (2008) 210.

[10] G. Bertuccio et al., *Study of silicon carbide for x-ray detection and spectroscopy, IEEE Trans. Nucl. Sci.* **50** (2003) 175.

[11] C. Cazzaniga et al., *A diamond based neutron spectrometer for diagnostics of deuterium–tritium fusion plasmas, Rev. Sci. Instrum.* **85** (2014) 11E101.

[12] A. Muraro et al., *First neutron spectroscopy measurements with a pixelated diamond detector at JET, Rev. Sci. Instrum.* **87** (2016) 11D833.

[13] M. Rebai et al., *Response function of single crystal synthetic diamond detectors to 1–4 MeV neutrons for spectroscopy of D plasmas, Rev. Sci. Instrum.* **87** (2016) 11D823.

[14] D. Rigamonti et al., *Neutron spectroscopy measurements of 14 MeV neutrons at unprecedented energy resolution and implications for deuterium-tritium fusion plasma diagnostics, Meas. Sci. Technol.* **29** (2018) 045502.

[15] M. Rebai et al., *Fission diamond detector tests at the ISIS spallation neutron source, Nucl. Phys. B Proc. Suppl.* **215** (2011) 313.

[16] L. Giacomelli et al., *Pulsed neutron beam measurements with diamond detectors, Nucl. Instrum. Methods Phys. Res., Sect. A* **720** (2013) 125.

[17] L. Giacomelli et al., *Neutron emission spectroscopy of DT plasmas at enhanced energy resolution with diamond detectors, Rev. Sci. Instrum.* **87** (2016) 11D822.

[18] M. Rebai et al., *New thick silicon carbide detectors: response to 14 MeV neutrons and comparison with single-crystal diamonds, Nucl. Instrum. Methods Phys. Res., Sect. A* **946** (2019) 162637.

[19] M.H. Kushoro et al., *Silicon carbide characterization at the n_TOF spallation source with quasi-monoenergetic fast neutrons, Nucl. Instrum. Methods Phys. Res., Sect. A* **983** (2020) 164578.

[20] M.H. Kushoro et al., *Detector response to D−D neutrons and stability measurements with 4H silicon carbide detectors*, *Materials* **14** (2021) 568.

[21] M. Rebai et al., *Time-stability of a single-crystal diamond detector for fast neutron beam diagnostic under alpha and neutron irradiation*, *Diamond Relat. Mater.* **61** (2016) 1.

[22] M. Hodgson et al., *Neutron detection performance of silicon carbide and diamond detectors with incomplete charge collection properties*, *Nucl. Instrum. Methods Phys. Res., Sect. A* **847** (2017) 1.

[23] J.H. Ha et al., *4H-SiC PIN-type semiconductor detector for fast neutron detection*, *Prog. Nucl. Sci. Technol.* **1** (2011) 237.

[24] R. Pilotti et al., *Development and high temperature testing by 14 MeV neutron irradiation of single crystal diamond detectors*, 2016 *JINST* **11** C06008.

[25] M. Angelone et al., *High temperature response of a single crystal CVD diamond detector operated in current mode*, *Nucl. Instrum. Methods Phys. Res., Sect. A* **943** (2019) 162493.

[26] S. Tudisco et al., *Silicon carbide for future intense luminosity nuclear physics investigations*, *Il Nuovo Cimento C* **42** (2019) 74.

[27] S. Tudisco et al., *SiCILIA-silicon carbide detectors for intense luminosity investigations and applications*, *Sensors* **18** (2018) 2289.

[28] F.H. Ruddy et al., *The fast neutron response of 4H silicon carbide semiconductor radiation detectors*, *IEEE Trans. Nucl. Sci.* **53** (2006) 1666.

[29] K. Sedlackova et al., *Properties of SiC semiconductor detector of fast neutrons investigated using MCNPX code*, *19th International Conference on Applied Physics of Condensed Matter* available on ResearchGate: https://www.researchgate.net/publication/284191754_Properties_of_SiC_ semiconductor_detector_of_fast_neutrons_investigated_using_MCNPX_code.

[30] https://www.nndc.bnl.gov/qcalc/.

[31] https://physics.nist.gov/PhysRefData/Star/Text/ASTAR.html.

[32] A. Meli et al., *Epitaxial growth and characterization of 4H-SiC for neutron detection applications*, *Materials* **14** (2021) 976.

[33] G.F. Knoll, *Radiation Detection and Measurement*, John Wiley & Sons, New York (2010).

[34] https://cividec.at/index.php?module=public.category&cat=5.

[35] https://www.caen.it/products/dt5730/.

[36] M. De Napoli, *SiC detectors: a review on the use of silicon carbide as radiation detection material*, *Front. Phys.* **10** (2022) 898833.

[37] F. La Via et al., *Mechanisms of growth and defect properties of epitaxial SiC*, *Appl. Phys. Rev.* **1** (2014) 031301.